This article was downloaded by:
On: *14 January 2011*
Access details: *Access Details: Free Access*
Publisher *Taylor & Francis*
Informa Ltd Registered in England and Wales Registered Number: 1072954 Registered office: Mortimer House, 37-41 Mortimer Street, London W1T 3JH, UK

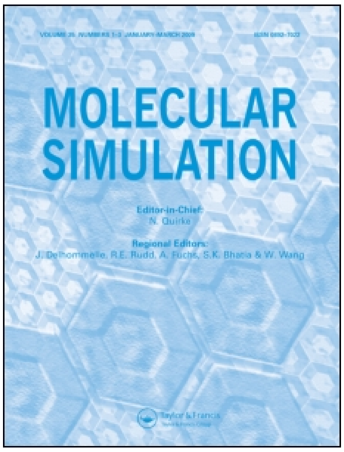

Molecular Simulation

Publication details, including instructions for authors and subscription information:
http://www.informaworld.com/smpp/title~content=t713644482

Theoretical Calculation of a Solution Phase Torsional Free Energy Profile. π-Ethylimidazole in Water

David R. Lowis[a]; Jonathan W. Essex[a]; W. Graham Richards[a]
[a] Physical Chemistry Laboratory, Oxford Centre for Molecular Sciences, Oxford, UK

To cite this Article Lowis, David R. , Essex, Jonathan W. and Richards, W. Graham(1993) 'Theoretical Calculation of a Solution Phase Torsional Free Energy Profile. π-Ethylimidazole in Water', Molecular Simulation, 9: 6, 369 — 383
To link to this Article: DOI: 10.1080/08927029308048268
URL: http://dx.doi.org/10.1080/08927029308048268

PLEASE SCROLL DOWN FOR ARTICLE

Full terms and conditions of use: http://www.informaworld.com/terms-and-conditions-of-access.pdf

This article may be used for research, teaching and private study purposes. Any substantial or systematic reproduction, re-distribution, re-selling, loan or sub-licensing, systematic supply or distribution in any form to anyone is expressly forbidden.

The publisher does not give any warranty express or implied or make any representation that the contents will be complete or accurate or up to date. The accuracy of any instructions, formulae and drug doses should be independently verified with primary sources. The publisher shall not be liable for any loss, actions, claims, proceedings, demand or costs or damages whatsoever or howsoever caused arising directly or indirectly in connection with or arising out of the use of this material.

Molecular Simulation, 1993, Vol. 9(6), pp. 369-383
Reprints available directly from the publisher
Photocopying permitted by license only

THEORETICAL CALCULATION OF A SOLUTION PHASE TORSIONAL FREE ENERGY PROFILE. π-ETHYLIMIDAZOLE IN WATER

DAVID R. LOWIS, JONATHAN W. ESSEX and W. GRAHAM RICHARDS

*Oxford Centre for Molecular Sciences, Physical Chemistry Laboratory,
South Parks Road, Oxford, OX1 3QZ, UK*

(Received May 1992, accepted May 1992)

Ab initio molecular orbital calculations, in conjunction with Monte Carlo statistical mechanics simulations, have been used to calculate the torsional free energy profile for π-ethylimidazole in aqueous solution. Geometry optimisations were carried out with 3–21G and 6–31G* basis sets on various conformational forms of π-ethylimidazole. Electron correlation energies were calculated from the 6–31G* optimised geometries using Møller-Plesset second order perturbation theory and single point calculations with the STO-3G basis set were used to obtain an estimate of atomic polarisation effects. Gas phase torsional energy barriers were found to be small; ~7–8 kJmol^{-1} for the principal barrier and ~4.5–5.5 kJmol^{-1} for the subsidiary barrier. Free energy perturbation theory was then applied in Monte Carlo simulations to examine the effect of solvation on the calculated gas phase torsional energy profile. The variable torsion angle of a single π-ethylimidazole molecule in a periodic box of 505 TIP4P water molecules was changed in discrete steps from 0° to 180° and the incremental free energy changes calculated. The calculated solution phase free energy results were of high precision and showed that solvation raised the principal torsional barrier ($\tau = 180°$) by 1.8 kJmol^{-1} and moved the subsidiary barrier from $\tau = 45°$ to $\tau = 0°$. The small free energy changes calculated were found to be the result of small differences between much larger enthalpy and entropy changes. Enthalpic and entropic effects were partly rationalised in terms of solute-solvent radial distribution functions although solvation effects were considerably more complex than expected.

KEY WORDS: Free energy perturbation, torsional free energy profile, π-ethylimidazole, Monte Carlo, radial distribution function.

INTRODUCTION

The mode of action of drug molecules in the body involves their binding to macromolecular receptors. If the nature of these drug-receptor interactions can be elucidated then, in principle, pharmacologically active molecules can be designed. One of the fundamental physical properties affecting binding is the compatibility of the receptor structure with the shape of the drug molecule. Hence, the thermally accessible conformations of the drug molecule will critically affect binding.

Experimental studies on small molecules in solution, such as n.m.r, look only at molecular conformations which have an appreciable population [1]; these are not necessarily the molecular shapes which are essential for binding at a particular receptor. Theoretical studies are not limited in this way, and can therefore be used to study all molecular conformations. Comparison of the thermally accessible conformations of related pharmacologically active molecules can enable the molecular shape essential for activity at a particular receptor to be found [2]. In the

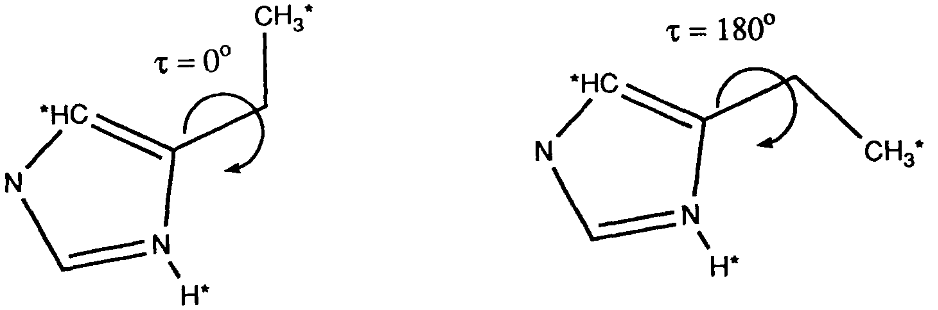

Figure 1 The above figure shows the two extreme conformations of π-ethylimidazole with $\tau = 0°$ and $\tau = 180°$. The CH united atom, (N) – H proton and methyl group mentioned in the discussion section are marked with asterisks.

past, such studies have involved the calculation of gas phase torsional energy profiles by *ab initio* [3] or semi-empirical [4] methods. Whilst this approach has met with considerable success the important effect of solvation has been neglected.

This paper outlines how gas phase *ab initio* calculations can be combined with the free energy perturbation (FEP) theory, in the context of Monte Carlo (MC) molecular simulations, to calculate a solution phase torsional molecular free energy profile, π-ethylmidazole was chosen as a simple test case as it possesses only one torsional degree of freedom which is similar to the τ_1 torsion in histamine, the value of which is thought to play a part in activity at the H_1 receptor [5].

METHOD

Ab Initio calculations

The Gaussian 88 program [6] was used to perform *ab initio* molecular orbital calculations on the Cray X-MP at the Rutherford Appleton Laboratory. Full geometry optimisations were carried out on thirteen different conformational forms of π-ethylimidazole at values of τ ranging from 0° to 180° (see Figure 1) in increments of 15°, at the 3–21G [7] and 6–31G* [8] basis set levels. The 6–31G* calculations were supplemented by the calculation of single point electron correlation energies via second order Møller-Plesset perturbation theory [9]. Finally, single point calculations were carried out on the 6–31G* optimised geometries at the minimal basis set, STO-3G [10], level to obtain an estimate of atomic polarisation effects [11].

MONTE CARLO SIMULATIONS

A series of MC statistical mechanical simulations were carried out on a system of one π-ethylimidazole molecule surrounded by 505 water molecules in a cubic box to which periodic boundary conditions were applied. The TIP4P model [12] was employed for solvent-solvent interactions whilst OPLS parameters [13] were used to describe π-ethylimidazole which was represented by eight united atoms.

Metropolis [14] and preferential samplling [15] were employed throughout all simulations. Spherical cut-offs for intermolecular interactions were applied at 9 Å for both solvent-solvent and solute-solvent interactions with the cut-off criterion such that if one atom of the solute lay within the cut-off then interactions with all other solute atoms were included in the calculation. Empirical parameters which determine the range of solute molecule movement and the size of system volume moves were optimised in a series of short test jobs to achieve solute move and volume move acceptance rates of around 40 per cent [16].

Free energy perturbation theory was used to calculate the change in the intermolecular contribution to the free energy as the $CH\text{-}C\text{-}CH_2\text{-}CH_3$ dihedral (see Figure 1) was increased from $\tau = 0°$ to $\tau = 180°$. Increments of 10° were used in order that the free energy changes calculated would have precise values. The free energy difference accompanying a change in τ from ρ_i to τ_j, where $\tau_j = \tau_i + \Delta\tau$, $\Delta\tau$ being equal to 10°, is given by equation (1) [17]. $E_j - E_i$ is the difference in solute-solvent interaction energies between systems τ_j and τ_i and the average, denoted by $< >_i$, is based on sampling over configurations of τ_i.

$$\Delta G = G_j - G_i = -kT \ln < \exp\left(-(E_j - E_i)/kT\right) >_i \tag{1}$$

If the value of $E_j - E_i$ is large, i.e. there is too great a disparity between reference, τ_i, and perturbed, τ_j, systems then equation (1) will be slow to converge [18]. For this reason small perturbation windows of 10° were used, and the Z-matrix describing the solute structure was set up such that the imidazole ring remained fixed whilst the ethyl side chain was moved in the perturbation. In a previous series of simulations the ethyl side chain was fixed and the imidazole ring twisted in increments of 15°. This generated free energy results with a significantly greater hysteresis and larger uncertainty than the data presented here. Moreover, this data gave the spurious result of altering the position of the global minimum from the gas phase value of $\tau = 105°$ to $\tau = 0°$. For this reason we emphasise that care must be taken in ensuring the convergence of equation (1).

The simulations were run using the BOSS program [19] on a Hewlett Packard 700 series computer. The BOSS program incorporates double wide sampling by monitoring three solutes simultaneously, the reference solute, τ_i and two perturbed solutes, $\tau_i \pm \Delta\tau$. Simulations were run with $\tau_i = 0°$, 10°, 20°, 30°, 40°, . . . 180° in order to obtain ΔG values for both forward and backward perturbations, i.e. $\tau_i \; -> \tau_j$ and $\tau_j - > \tau_i$.

Each simulation consisted of 2.3×10^6 configurations of equilibration, the first 3×10^5 of which were at constant volume, followed by 4×10^6 configurations of data collection. A total of 119.7×10^6 configurations were utilised altogether, all calculations being run in the isothermal-isobaric (constant NPT) ensemble at 25°C and 1 atmosphere pressure.

RESULTS AND DISCUSSION

Ab Initio calculations

The results of the *ab initio* calculations on π-ethylimidazole are recorded in Table 1; results from the 3–21G, 6–31G* optimisations and MP2 corrections to the 6–31 g* calculations are also displayed in Figure 2. The torsional functions calculated using these basis sets all have similar profiles with the main discrepancies being in

Table 1 *Ab initio* energies as a function of the torsional angle, τ, of π-ethylimidazole. The final column shows the results of the fitting of an 8th order polynomial (equation (3), below) to the MP2/6–31G*// RHF/6–31G* results.

	Ab initio energy/kJmol^{-1}				
tor	RHF/3.21G// RHF/3-21G	RHF/6.31G*// RHF/6-31G*	RHF/STO-3G// RHF/6-31G*	MP2/6-31G*// RHF/6-31G*	8th order polynomial fit/kJmol^{-1}
0	1.773	0.612	1.800	1.327	1.341
15	2.418	1.188		1.627	1.525
30	3.937	2.623	2.578	2.497	2.794
45	5.328	4.144		4.581	4.146
60	5.274	4.657	2.881	3.834	4.122
75	3.886	3.451		2.714	2.708
90	1.530	1.462	0.586	1.009	0.955
105	0.000	0.019		0.000	−0.054
120	0.097	0.000	0.000	0.079	0.117
135	1.840	1.525		1.228	1.304
150	4.569	4.194	3.730	3.369	3.269
165	7.036	6.899		5.762	5.807
180	8.027	8.806	5.954	6.933	6.926

$$\begin{aligned} f(x) = & -6.0135597014\times 10^{15}x^{8}+4.4637337668\times 10^{12}x^{7} \\ & -1.3197508730\times 10^{-9}x^{6}+ \\ & 1.9888253767\times 10^{-7}x^{5}-1.5656156755\times 10^{-5}x^{4} \\ & +5.7823793113\times 10^{-9}x^{3}-7.1539506356\times 10^{-3}x^{2}+3.320458564x \\ & -1.341201321 \end{aligned} \tag{3}$$

the exact positions of the global minimum ($\tau = 105°/120°$) and subsidiary maximum ($\tau = 45°/60°$), the energy of the subsidiary minimum ($\tau = 0°$) and the heights of the torsional barriers. The lowest torsional barriers were, as expected, found from the MP2/6–31G*//RHF/6–31G* calculations which take account of electron correlation, although all calculations predicted very low barriers of around 7 to 8 kJmol^{-1} ($\tau = 180°$) and around 4.5 to 5.5 kJmol^{-1} ($\tau = 45°$). Interestingly, the MP2/6–31G*//RHF/6–31G* calculations predict a higher energy at the subsidiary minimum, $\tau = 0°$, than do the equivalent calculations neglecting electron correlation.

The overall shape of the gas phase torsional energy profile results from a combination of electronic, steric and polarisation effects; rationalisation of the computed torsional barriers of π-ethylimidazole was found to be impossible using any simple argument. Results from the single point minimal basis set, RHF/STO-3G//RHF/STO-3G, calculations are displayed along with those from the other *ab initio* calculations in Figure 2. The STO-3G basis set does not include polarisation functions and thus the difference between these STO-3G and the 6–31G* results gives an estimate of the magnitude of atomic polarisation effects [11]. The STO-3G torsional barriers were found to be some 1.5–2 kJmol^{-1} lower than those calculated using the 6–31G* basis set, implying that atomic polarisation contributes approximately 2 kJmol^{-1} to the principal torsional barrier $\tau = 180°$) and 1.5 kJmol^{-1} to the subsidiary torsional barrier ($\tau = 45°$).

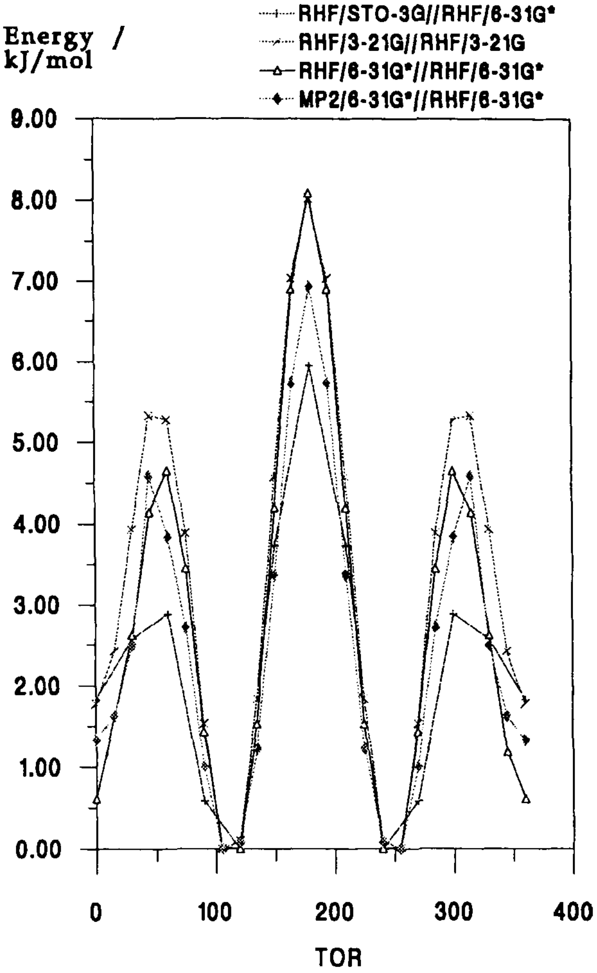

Figure 2 *Ab initio* energies.

MONTE CARLO SIMULATIONS

The incremental free energy changes, ΔΔG, are recorded in Table 2 along with their accumulated total, ΔG, and the results from the fitting of an 8th order polynomial (equation (3), given under Table 1) to the data obtained from the MP2/6–31G*//RHF/6–31G* *ab initio* calculations, ΔE_{gas}. The curve fitted to the MP2/6–31G*//RHF/6–32G* results showed a close fit with the maximum deviation from the *ab initio* results being 0.4 kJmol^{-1} at $\tau = 45°$. The zero of energy for the solution phase results was taken from the 6–31G* gas phase minima at $\tau = 120°$. The simulations undertaken combined with the implementation of double wide sampling within the BOSS program provided two independent evaluations of the effects of solvation on the gas phase torsional energy profile. Figure 3 shows the

Table 2 Incremental free energy changes, ΔΔG, for both $\tau_i \rightarrow \tau_j$ and $\tau_j \rightarrow \tau_i$ $\Delta G_{av,acc}$ denotes the average of $\Delta\Delta G_{\tau_j \rightarrow \tau_i}$ and $\Delta\Delta G_{\tau_i \rightarrow \tau_j}$ accumulated to τ_i ΔE_{gas} shows the results of the fitting of an 8th order polynomial (equation (3) see caption under Table 1) to the MP2/6–31G*/RHF/6–31G* *ab initio* calculations and $W(\tau)$ is the torsional potential of mean force for π-ethylimidazole in aquous solution as found from equation (2).

		$\Delta\Delta G$/kJmol^{-1}				
τ_i	τ_j	$\tau_j \rightarrow \tau_i$	$\tau_j \rightarrow \tau_i$	$\Delta G_{av.acc}$ for τ_i /kJmol^{-1}	ΔE_{gas} for τ_i /kJmol^{-1}	$W(\tau)$ for τ_i /kJmol^{-1}
0	10	0.04 ±0.03	0.00 ±0.02	−0.08	1.34	1.26
10	20	0.00 ±0.03	0.05 ±0.04	−0.01	1.40	1.39
20	30	−0.00 ±0.04	0.05 ±0.04	−0.09	1.82	1.73
30	40	0.00 ±0.03	0.04 ±0.05	−0.19	2.79	2.60
40	50	−0.01 ±0.05	−0.15 ±0.05	−0.28	3.80	3.52
50	60	0.19 ±0.05	−0.09 ±0.07	0.02	4.32	4.34
60	70	0.06 ±0.072	0.09 ±0.043	0.59	4.12	4.71
70	80	−0.05 ±0.05	0.04 ±0.05	0.54	3.28	3.82
80	90	−0.03 ±0.05	0.04 ±0.04	0.34	2.10	2.44
90	100	−0.06 ±0.03	0.09 ±0.04	0.21	0.96	1.17
100	110	0.02 ±0.04	0.02 ±0.05	−0.10	0.16	0.06
110	120	0.02 ±0.04	−0.03 ±0.05	−0.09	−0.13	−0.22
120	130	0.02 ±0.05	−0.10 ±0.07	0.00	0.12	0.12
130	140	0.07 ±0.06	−0.02 ±0.08	0.26	0.81	1.07
140	150	−0.03 ±0.06	−0.15 ±0.05	0.45	1.88	2.33
150	160	0.11 ±0.06	−0.21 ±0.10	0.70	3.27	3.97
160	170	0.09 ±0.07	−0.02 ±0.04	1.38	4.94	6.32
170	180	−0.00 ±0.06	−0.09 ±0.04	1.63	6.57	8.20
180				1.81	6.93	8.73

results of these independent evaluations. The trends displayed in the results from these two runs are very similar, shown by the small difference in ΔG values, at $\tau = 0°$, of ~0.3 kJmol^{-1} indicating that sampling of phase space within the simulations has been efficient. The standard deviations on individual ΔΔG values provide an estimate of the errors involved in their calculation; the standard deviations on ΔΔG values given in Table 2 are small, demonstrating the high precision of the computed solution phase free energies. The τ dependence of the free energy of hydration of π-ethylimidazole was calculated by averaging the results from the independent BOSS calculations and is illustrated in Figure 4 along with the curve fitted to the MP2/6-31G*/RHF/6-31G* *ab initio* results and the torsional potential ot mean force, $W(\tau)$. The torsional potential of mean force, $W(\tau)$ for π-ethylimidazole in aqueous solution was calculated from equation 2 [20] by the addition of ΔG, the free energy of hydration as a function of τ, to the 6-31G*/MP2 *ab initio* results and is given in Table 2.

$$W(\tau) = \Delta G + \Delta E_{gas} \tag{2}$$

A general decrease in the free energy of hydration of π-ethylimidazole is evident as τ is decreased from 180° to 0° although a number of features are superimposed upon this. Most evident are peaks at $\tau = 180°$ and 60° which correlate with those in

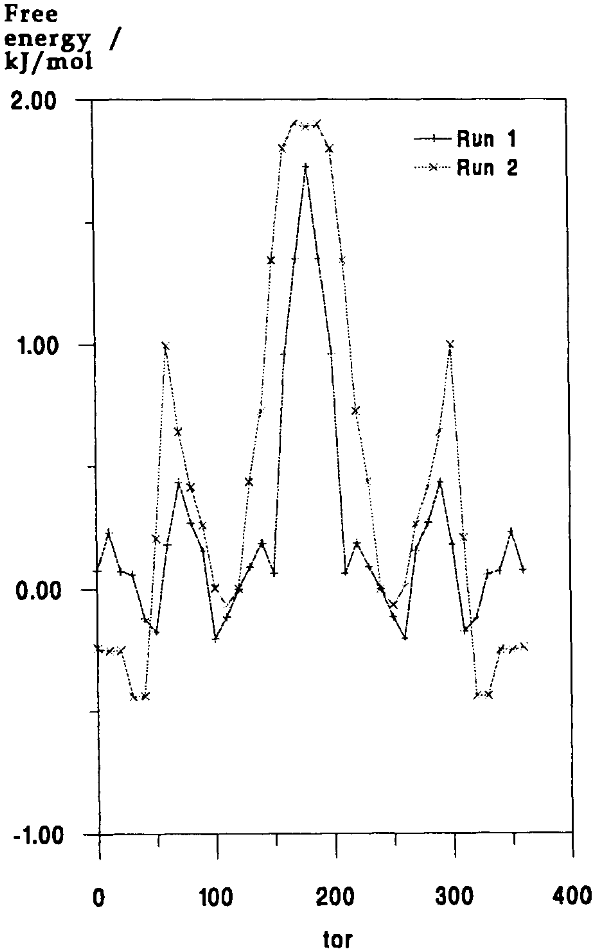

Figure 3 Solution phase free energy results for runs 1 and 2. Free energy results for run 1 were obtained from simulations performed at 0°, 20°, 40°, . . ., 180° whilst run 2 free energy results were obtained from simulations performed at 10°, 30°, 50°, . . ., 170°. With the implementation of double wide sampling in the BOSS program the entire $\tau = 0°$ to 180° range was covered in both sets of simulations.

the gas phase profile, and troughs at $\tau = 120°$ and $\tau = 40°$. The main effects of hydration on the gas phase torsional energy profile are the raising of the principal torsional barrier at $\tau = 180°$ by $\sim 1.8\,\mathrm{kJmol^{-1}}$ and the shift of the subsidiary barrier from $\tau = 45°$ to $\tau = 60°$, the relative energies of the two gas phase minima remaining effectively constant.

Values for the incremental enthalpy, $\Delta\Delta H$, and entropy, $\Delta\Delta S$, changes as τ is perturbed from 0° to 180° are also calculated by the BOSS program; these results are given in Table 3 and illustrated in Figure 5. $\Delta\Delta H$ values are calculated using umbrella sampling and the Gibbs-Helmholtz equation. Owing to the method of calculation of $\Delta\Delta H$ and $\Delta\Delta S$, errors on these figures are much greater than those for incremental free energy changes; this can be seen from the standard deviations in Table 3. However, despite the large uncertainty in these results, the gross

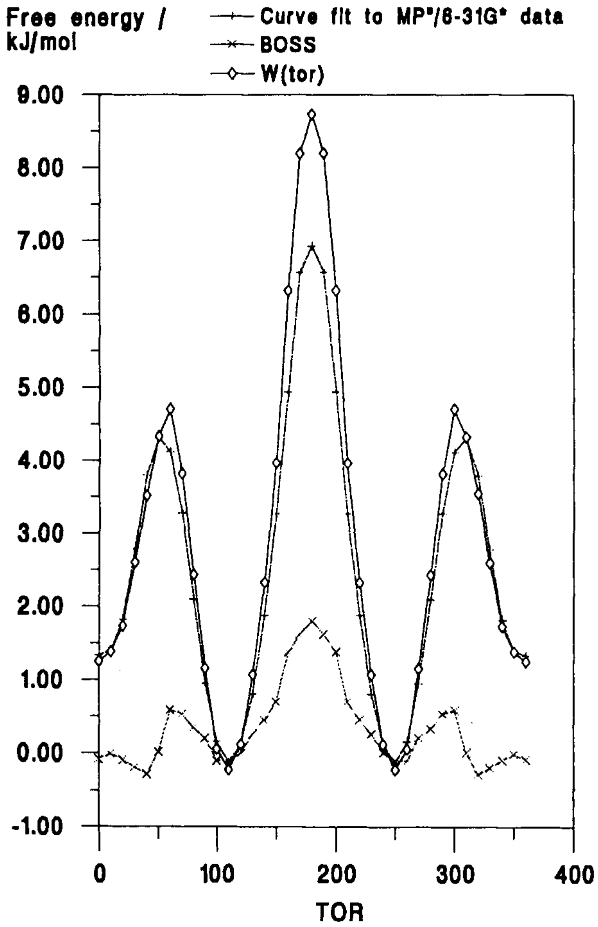

Figure 4 Total potential of mean force, $W(\tau)$ for π-ethylimidazole in aqueous solution. Also displayed are the averaged solution phase free energy results, ΔG, and the results, ΔE_{gas}, from fitting an 8th order polynomial to the MP2/6-31G*//RHF/6-31G* *ab initio* data.

Table 3 Values for incremental enthalpy, $\Delta\Delta H$, and entropy, $\Delta\Delta S$, $\Delta H_{av,acc}$ denotes the average of $\Delta\Delta H_{\tau_i \to \tau_j}$ and $\Delta\Delta H_{\tau_j \to \tau_i}$ accumulated to τ_i, whilst $\Delta S_{av,acc}$ denotes the average of $\Delta\Delta S_{\tau_i \to \tau_j}$ and $\Delta\Delta S_{\tau_j \to \tau_i}$ accumulated to τ_i.

τ_i	τ_j	$\Delta\Delta H$ /kJmol^{-1}		$\Delta\Delta S$ /JK^{-1}mol^{-1}		$\Delta H_{av.acc}$ for τ_i /kJmol^{-1}	$\Delta S_{av.acc}$ for τ_i /JK^{1}mol^{-1}
		$\tau_i \to \tau_j$	$\tau_j \to \tau_i$	$\tau_i \to \tau_j$	$\tau_j \to \tau_i$		
0	10	−12.18 ±5.44	−1.90 ±2.05	−41.37 ±17.92	−4.66 ±6.70	−0.64	−2.60
10	20	1.21 ±2.14	1.58 ±5.23	4.05 ±6.87	4.77 ±17.42	−5.78	−20.96
20	30	−4.99 ±4.50	13.32 ±4.98	−16.69 ±15.40	44.07 ±16.61	−5.97	−21.32
30	40	−15.25 ±4.29	9.38 ±5.84	−51.15 ±14.28	30.84 ±19.90	−15.12	−51.70
40	50	−6.53 ±5.08	2.72 ±5.48	−31.73 ±17.15	11.27 ±18.38	−27.44	−92.69
50	60	4.17 ±6.19	−23.55 ±10.22	11.34 ±20.99	−77.80 ±34.03	−32.06	−109.19
60	70	21.42 ±11.04	0.98 ±6.25	79.97 ±37.06	2.08 ±20.83	−18.20	−64.62
70	80	1.63 ±5.90	−7.90 ±6.40	9.39 ±19.69	−27.06 ±21.27	−7.98	−30.18
80	90	13.01 ±7.69	−28.90 ±414.46	44.01 ±25.83	−97.46 ±48.12	−3.22	−11.95
90	100	6.66 ±6.60	6.82 ±3.48	23.20 ±22.00	21.68 ±11.91	7.74	58.79
100	110	−9.45 ±3.19	10.79 ±7.18	−32.00 ±10.66	35.95 ±24.09	17.66	59.55
110	120	−2.10 ±3.79	12.97 ±6.51	−7.25 ±12.86	43.90 ±22.01	7.54	25.58
120	130	−8.17 ±4.17	1.95 ±6.66	−27.70 ±14.08	8.00 ±22.31	0.00	0.00
130	140	−3.11 ±6.14	−1.90 ±7.70	−11.40 ±20.65	−6.07 ±25.65	−5.06	−17.85
140	150	7.46 ±14.08	−7.81 ±5.09	25.43 ±47.50	−24.12 ±17.09	−5.67	−20.52
150	160	5.56 ±5.28	−11.65 ±10.29	17.13 ±17.49	−36.08 ±33.94	1.97	4.26
160	170	−4.83 ±5.84	−10.75 ±4.81	−17.47 ±19.71	−35.70 ±16.25	10.58	30.87
170	180	15.62 ±7.09	−6.25 ±4.18	52.43 ±24.24	−19.70 ±13.90	13.54	39.98
180						24.47	76.05

features observed are statistically significant. Insight into the role of differing solvation effect on the free energy of hydration of π-ethylimidazole as τ is mutated from 0° to 180° may be gained from examination of the ΔH, $T\Delta S$ plots. Many of these features can be rationalised in terms of the solute-solvent radial distribution functions.

The radial distribution functions for the united atom CH group, the (N) − H proton and the methyl group with water oxygen atoms are shown, for $\tau = 0°$ and 60° in parts A, B and C of Figure 6 respectively. The numbers in the top left hand corners of these plots denote the number of water oxygen atoms in the first solvation shell of the corresponding functional group, the cut-off being taken from

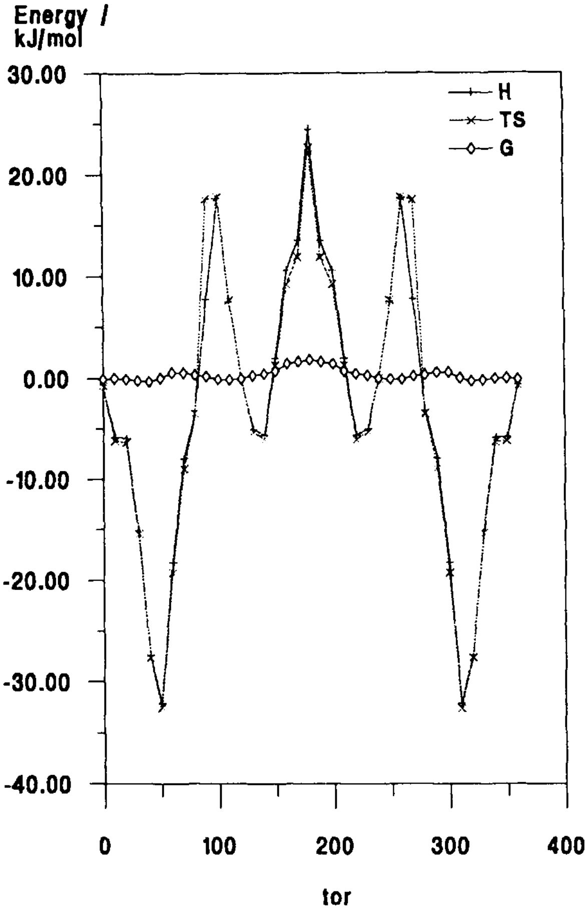

Figure 5 The dependance of the intermolecular enthalpy, ΔH, and entropy, illustrated here as TΔS, of π-ethylimidazole on the variable torsion angle τ. Also shown is the free energy of hydration, ΔG, as a function of τ.

the solid vertical line. The solute-solvent radial distribution functions for the CH united atom with water oxygen atoms (OW), Figure 6A, show little change in solvent order as τ is changed from 0° and 60°. If the first solvation shell is assumed to terminate at 4.5 Å, then the number of water molecules in this solvation shell is very similar for both the $\tau = 0°$ and the $\tau = 60°$ conformations. These two factors do not discriminate between the $\tau = 0°$ and $\tau = 60°$ conformations on either enthalpic or entropic grounds to any reasonable extent. Examination of the (N)-H proton, OW radial distribution functions at $\tau = 0°$ and $\tau = 60°$, Figure 6B, shows greater solvent order at $\tau = 0°$; this function has a higher initial peak (at ~2 Å), a lower initial trough (at ~2.5 Å) and shows the existence of four solvation shells, at 2, 4, 6 and 8 Å. The number of water molecules contained in the first solvation shell of (N) – H is practically identical for both $\tau = 0°$ and $\tau = 60°$. Considering the (N)-H radial distribution function data, enthalpic solvation effects appear

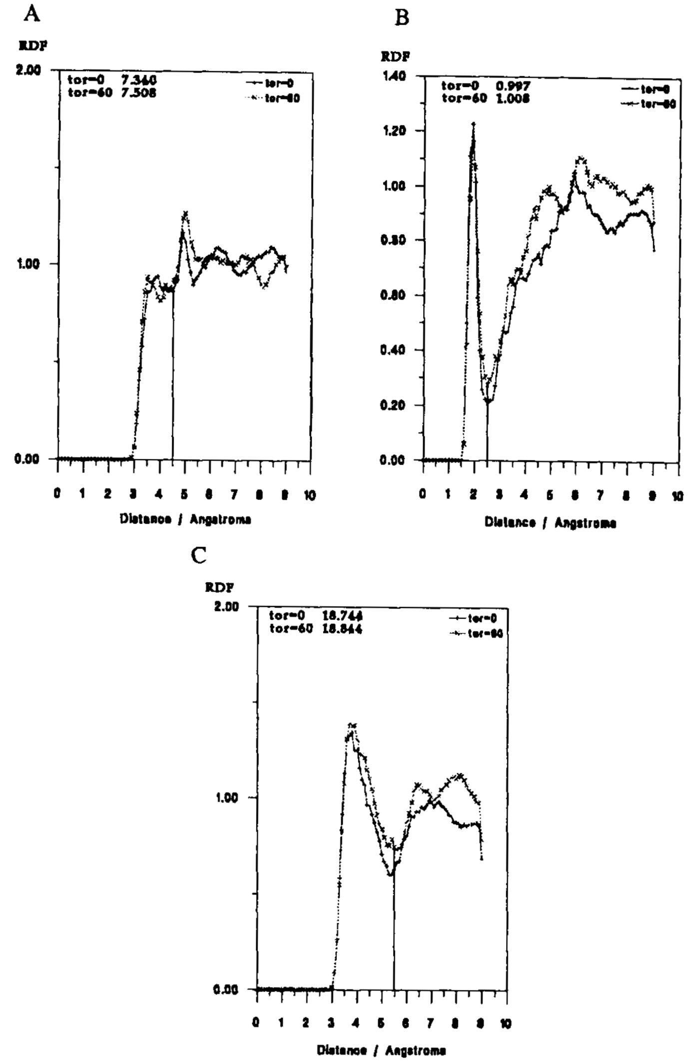

Figure 6 Solute-solvent radial distribution functions at $\tau = 0°$ and $\tau = 60°$ of the CH united atom, (N)-H proton and CH_3 group, parts A, B and C respectively. The numbers in the top left hand corners of each plot denote the number of water molecules in the first solvation shell of each group, the cutoff being taken from the vertical lines illustrated on each plot.

negligible but the $\tau = 60°$ conformation is marginally favoured on entropic grounds. Solvation of the methyl group in the $\tau = 0°$ conformation appears, from Figure 6C, to be more ordered than that of the $\tau = 60°$ conformation, tending to favour the $\tau = 60°$ conformation on entropic grounds. The difference in the number of water molecules in the first solvation shells of both conformations is very small making any enthalpic distinction between the conformations negligible. Overall, when considering the changes in solvation of the various groups on increasing τ from 0° to 60° the predominant effects will expected to be due to the solvation of the methyl group and the CH united atom. It has already been seen, however, that the solvation of the CH united atom alters little. Therefore, it is the solvation changes around the CH_3 group which should predominantly determine the change in the free energy of hydration of π-ethylimidazole between $\tau = 0°$ and $\tau = 60°$. In this respect the solute-solvent radial distribution function data does not correlate with the ΔH, $T\Delta S$ plots shown in Figure 5. The ΔH, $T\Delta S$ plots show the $\tau = 60°$ conformer to be enthalpically favoured and entropically disfavoured whilst the RDF data indicates little enthalpic difference between the two conformers and that the $\tau = 60°$ conformer should be favoured on entropic grounds.

Solvent-solvent radial distribution functions were also generated, these allow interpretation of the measured free energy changes in terms of the behaviour of bulk solvent. The solvent-solvent radial distribution functions calculated at various values of τ showed negligible differences indicating that any variation in the structure of the bulk solvent with increasing τ is small. The observed changes in enthalpy and entropy on going from $\tau = 0°$ to $\tau = 60°$ are consistent with a classical hydrophobic effect [21] as the solvent accessible surface area of the hydrophobic CH_3 group increases. Although bulk solvent structure was seen to remain unchanged as τ was increased, solvent structure in the region of the solute may show some dependence on the torsional angle τ; any structural change, however, would be swamped by the large amount of solvent further from the solute molecule.

Figure 7, parts A, B and C, show the radial distribution functions, with water oxygen atoms, of the CH united atom, (N)-H proton and CH_3 group respectively for $\tau = 120°$ and $\tau = 180°$. The solute-solvent radial distribution functions for the CH united atom, Figure 7A, show an increase in solvent order as τ is changed from 180° to 120°; this is shown by the higher initial peak in the $\tau = 120°$ radial distribution function. If the first solvation shell of the CH united atom is again assumed to terminate at 4.5 Å from the atom centre, then it can be seen that one more water molecule is contained within it when $\tau = 120°$ compared with the $\tau = 180°$ conformation. The ordering of solvent around the CH united atom at these values of τ tends to disfavour the 120° conformation on entropic grounds. However, owing to the greater number of solvent molecules in the first CH solvation shell the $\tau = 120°$ conformation is enthalpically favoured. Examination of the (N)–H proton, OW radial distribution functions at $\tau = 120°$ and $\tau = 180°$, Figure 7B, shows greater solvent ordering for the former conformation; the radial distribution function for the $\tau = 120°$ form has a higher initial peak and shows the existence of four discrete solvent shells at 2, 4, 6, and 9 Å. Approximately 0.15 more water molecules are contained in the first solvation shell of the (N)–H proton when $\tau = 120°$, in comparison with the $\tau = 180°$ conformation. Although this difference is small, it will still provide an enthalpic distinction between the two conformations since the water molecules in the first solvation shell of the (N)–H proton are more strongly bound than those in the first solvation shells of the hydrophobic methyl or CH groups. Hence, for the (N)–H proton radial distribution function data, entropic solvation effects disfavour the $\tau = 120°$ conformer; enthalpically, however, this conformer is favoured. Solvation of the methyl group in the $\tau = 120°$ conformation appears, from Figure 7C, to be more ordered than that of the $\tau = 180°$ conformation, again tending to entropically disfavour the former. The number of water molecules in the first solvation shell of the methyl group drops by approximately 1.5 on increasing τ from 120° to 180°, enthalpically

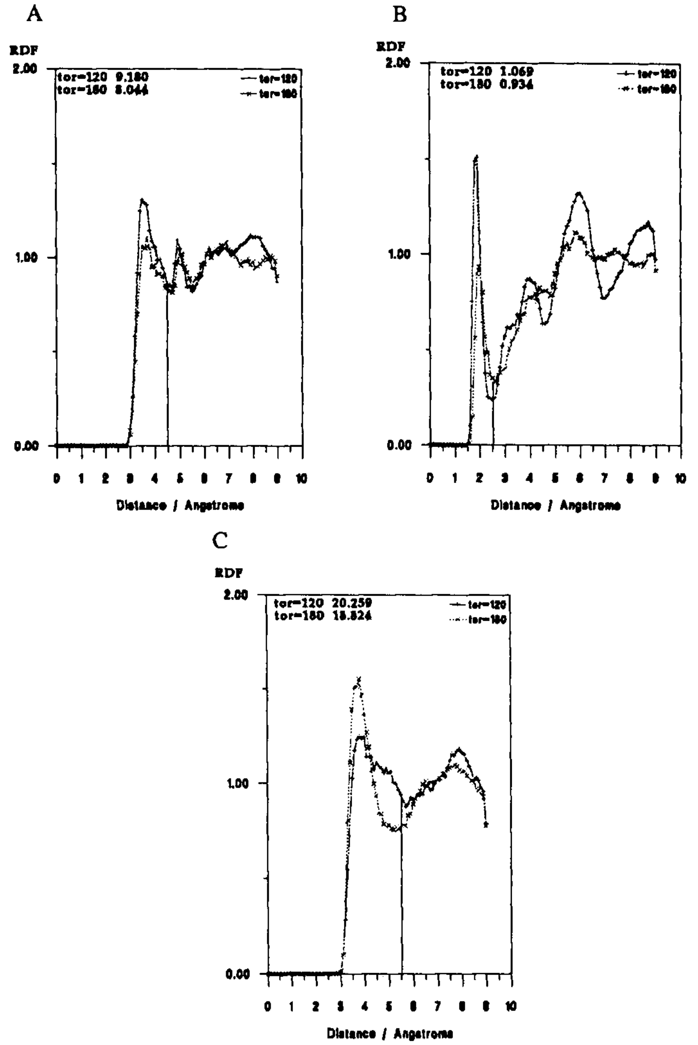

Figure 7 Solute-solvent radial distribution functions at $\tau = 120°$ and $\tau = 180°$ of the CH united atom, (N)-H proton and CH_3 group, parts A, B and C respectively. The numbers in the top left hand corners of each plot denote the number of water molecules in the first solvation shell of each group, the cutoff being taken from the vertical lines illustrated on each plot.

favouring the 120° conformer. It is expected, when considering conformations of π-ethylimidazole with $\tau = 120°$ and $\tau = 180°$, that the most important solvation effects will be due to variation in solvent structure around the methyl group and the (N)-H proton. Overall the solute-solvent radial distribution function data from all three functional groups shows the $\tau = 120°$ conformer of π-ethylimidazole to be enthalpically favoured but entropically disfavoured over the $\tau = 180°$ conformer. This is in qualitative agreement with the calculated enthalpy and entropy information.

No attempt has been made to rationalise the complex enthalpy and entropy behaviour observed between $\tau = 60°$ and $\tau = 120°$; any rationalisation in terms of solute-solvent radial distribution functions appears impossible.

CONCLUSION

The complete solution phase torsional potential of mean force for π-ethylimidazole in aqueous solution has been calculated. The results of the gas phase *ab initio* calculations reveal a complex torsional energy function containing two small barriers. The shape of the computed energy profile could not be rationalised by employing any simple steric, electronic or polarisation argument and must therefore be the result of a combination of these effects. Results from the single point STO-3G calculations, on 6–31G* optimised geometries, estimate the effects of atomic polarisation to be approximately of 2.1 $kJmol^{-1}$ to the principal torsional barrier, $\tau = 180°$, and 1.8 $kJmol^{-1}$ to the subsidiary torsional barrier. Calculation of electron correlation energies, via Møller-Plesset second order perturbation theory, reduced the calculated 6–31G* principal torsional energy barrier by 1.15 $kJmol^{-1}$.

The solution phase free energy results were calculated to high precision, as shown by the small standard deviations on individual $\Delta\Delta G$ values (Table 2), and clearly show the effects of solvation on the *ab initio* gas phase energy profile. The major changes to the gas phase torsional energy profile upon solvation are the raising of the principal torsional barrier, at $\tau = 180°$, by 1.81 $kJmol^{-1}$ and the shift of the subsidiary torsional barrier from the gas phase value of $\tau = 45°$ to a new value of $\tau = 60°$.

The behaviour of ΔH and ΔS as τ was increased from 0° to 180° is more complex than was first expected and for many values of τ large enthalpic and entropic effects virtually cancel. Rationalisation of these effects in terms solute-solvent radial distribution functions was only partially successful. Solvent-solvent radial distribution functions gave little indication of the changes in solvent structure as τ was increased from 0° to 180°; this is not unsurprising given that changes in solvent structure close to the solute would be swamped by the great expanse of solvent molecules in the bulk.

Although the effect of solvation on the thermally accessible conformations was minimal for this particular system, we can assert that in the case of charged or hydrophilic side chains, solvation will play a major role. Moreover, unless care is taken in performing the perturbations any results obtained will be misleading.

Given the earlier success of the OPLS parameter set in conjunction with Monte Carlo simulation in predicting the effect of solvation on conformational energy profiles [20] [22], there seems little doubt that the solvation effects observed in the case of π-ethylimidazole are real. Their interpretation, however, is problematic.

Acknowledgement

D.R.L would like to acknowledge the financial assistance of Lilly Research as part of a C.A.S.E. studentship. J.W.E would like to acknowledge the generous support of Glaxo Group Research in the form of a Glaxo Research Scholarship.

References

[1] R. Freeman, *A handbook of nuclear magnetic resonance spectroscopy*, Longman group UK Ltd (1988).

[2] W.G. Richards, *Quantum Pharmacology*, Butterworths, London (1983).

[3] O. Tapia, R. Cardenas, Y.G. Smythers, A. Hernandez-Laguna, J.J. Randez and F.J. Randez, "Exploring the potential energy hypersurface of histamine monocation", *International Journal of Quantum Chemistry*, **38**, 727 (1990).

[4] C.R. Ganellin, E.S. Pepper, G.N.J. Port and W.G. Richards, "Conformation of histamine derivatives. 1. Application of Molecular Orbital Calculations and n.m.r. Spectroscopy", *J. Med. Chem.*, **16**, 610 (1973).

[5] W.G. Richards, in *Proceedings of the 6th symposium on medicinal chemistry*, Brighton, UK. Sept 4–7 (1978)

[6] M.J. Frisch, M. Head-Gordon, H.B. Schlegel, K, Raghavachari, J.S. Binkley, C. Gonzalez, D.J. Defrees, D.J. Fox, R.A. Whiteside, R. Seeger, C.F. Melius, J. Baker, R. Martin, L.R. Khann, J.J.P. Stewart, E.M. Fluder, S. Topiol and J.A. Pople, *Gaussian 88*, Gaussian Inc., Pittsburgh, PA, USA (1988).

[7] J.S. Binkley, J.A. Pople and W.J. Hehre, *J. Am. Chem. Soc.*, **28**, 213 (1980).

[8] P.C. Hariharan and J.A. Pople, *Theor. Chim. Acta.*, **28**, 213 (1973).

[9] C. Møller and M.S. Plesset, "Notes on an approximation treatment for many electron systems", *Phys. Rev.*, **46**, 1381 (1985).

[10] W.J. Hehre, R.F. Stewart and J.A. Pople, "Self consistent molecular orbital methods I. Use of Gaussian expansions of Slater type atomic orbitals", *J. Chem. Phys.*, **51**, 2657 (1969).

[11] J.B. Collins, P.V.R. Schleyer, J.S. Binkley and J.A. Pople, "Self consistent molecular orbital methods XVII. Geometries and binding energies of second row molecules. A comparison of three basic sets", *J. Chem. Phys.*, **64**, 5142 (1976).

[12] W.L. Jorgensen, J. Chandresekhar, J.D. Madura, R.W. Impey and M.L. Klein, "Comparison of simple potential functions for simulating liquid water", *J. Chem. Phys.*, **79**, 926 (1983). W.L. Jorgensen and Madura J.D. *Mol. Phys.*, **56**, 1381 (1985).

[13] W.L. Jorgensen and J. Tirado-Rives, "The OPLS potential functions for proteins. Energy minimisations for crystals of cyclic peptides and crambin", *J. Am. Chem. Soc.*, **110**, 1657 (1988).

[14] N. Metropolis and S. Ulam, "The Monte Carlo Method", *J. Am. Stat. Ass.*, **44**, 335 (1949).

[15] W.L. Jorgensen, "Theoretical studies of medium effects on conformational equilibria", *J. Phys. Chem.*, **87**, 5311 (1983).

[16] I.R. McDonald, "NPT ensemble Monte Carlo calculations for binary liquid mixtures", *Mol. Phys.*, **23**, 41 (1972).

[17] R.W. Zwanzig, "High temperature equation of state by a perturbation method. 1. Non-polar gases", *J. Chem. Phys.*, **22**, 1420 (1954).

[18] C.A. Reynolds, in *Computer aided molecular design*, IBC, London (1989).

[19] W.L. Jorgensen, *BOSS* (version 2.8), Dept of Chemistry, Purdue University, West Lafayette, PA, USA (1990).

[20] W.L. Jorgensen and J.K. Buckner, "Use of statistical perturbation theory for computing solvent effects on molecular conformation. Butane in water", *J. Phys. Chem.*, **91**, 6083 (1987).

[21] F. Franks, "The hydrophobic interaction", in *Water*, Volume 4, Plenum Press, New York (1975).

[22] W.L. Jorgensen and J. Gao, "Cis/trans energy difference for the peptide bond in the gas phase and Aqueous solution", *J. Am. Chem. Soc.*, **110**, 4212 (1988).

APPENDIX

The BOSS intermolecular interreaction potential function.

$$V_{total} = \sum_{i=1}^{N_A} \sum_{j=i}^{N_A} \left\{ \varepsilon^*_{ij} \left[\left(\frac{R^*_{ij}}{R_{ij}} \right)^{12} - \left(\frac{R^*_{ij}}{R_{ij}} \right)^{6} \right] + \frac{q_i q_j}{\varepsilon R_{ij}} \right\}$$

Van der Waals Coulombic